Inorganic Chemistry

Article

pubs.acs.org/IC

Triamidetriamine Bearing Macrobicyclic and Macrotricyclic Ligands: Potential Applications in the Development of Copper-64 Radiopharmaceuticals

Kel Vin Tan,[†] Paul A. Pellegrini,[‡] Brian W. Skelton,[§] Conor F. Hogan,[†] Ivan Greguric,[‡] and Peter J. Barnard*[,†]

[†]Department of Chemistry, La Trobe Institute for Molecular Science, La Trobe University, Victoria 3086, Australia

[‡]ANSTO LifeSciences, Australian Nuclear Science and Technology Organisation, Menai, New South Wales 2234, Australia

[§]Centre for Microscopy, Characterisation and Analysis, The University of Western Australia, 35 Stirling Highway, Crawley, Western Australia 6009, Australia

Supporting Information

ABSTRACT: A versatile and straightforward synthetic approach is described for the preparation of triamide bearing analogues of sarcophagine hexaazamacrobicyclic cage ligands without the need for a templating metal ion. Reaction of 1,1,1-*tris*(aminoethyl)ethane (tame) with 3 equiv of 2-chloroacetyl chloride, yields the *tris*(α-chloroamide) synthetic intermediate **6**, which when treated with either 1,1,1-*tris*(aminoethyl)ethane or 1,4,7-triazacyclononane furnished two novel triamidetriamine cryptand ligands (**7** and **8** respectively). The Co(III) and Cu(II) complexes of cryptand **7** were prepared; however, cryptand **8** could not be metalated. The cryptands and the Co(III) complex **9** have been characterized by elemental analysis, ^{1}H and ^{13}C NMR spectroscopy, and X-ray crystallography. These studies confirm that the Co(III) complex **9** adopts an octahedral geometry with three facial deprotonated amido-donors and three facial amine donor groups. The Cu(II) complex **10** was characterized by elemental analysis, single crystal X-ray crystallography, cyclic voltammetry, and UV−visible absorption spectroscopy. In contrast to the Co(III) complex (**9**), the Cu(II) center adopts a square planar coordination geometry, with two amine and two deprotonated amido donor groups. Compound **10** exhibited a quasi-reversible, one-electron oxidation, which is assigned to the $Cu^{2+/3+}$ redox couple. These cryptands represent interesting ligands for radiopharmaceutical applications, and **7** has been labeled with ^{64}Cu to give ^{64}Cu-**10**. This complex showed good stability when subjected to L-cysteine challenge whereas low levels of decomplexation were evident in the presence of L-histidine.

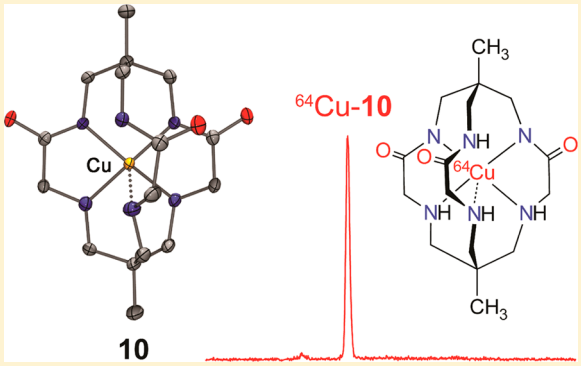

INTRODUCTION

Copper-64 is a promising radionuclide for positron emission tomography (PET) imaging. It is not only a positron-emitter (19%, $E_{\beta^+\,max}$ = 656 keV) but also a β^--emitter (39.6%, $E_{\beta^-\,max}$ = 573 keV) with a half-life of 12.7 h and may therefore be used for diagnostic and therapeutic applications.[1] Numerous chelating ligand systems have been evaluated for the development of ^{64}Cu-based PET imaging agents, and several excellent reviews exist.[1−5] The chemistry of Cu in vivo is complicated by the potential for bioreduction, where Cu(II) is reduced to Cu(I) followed by transchelation, and this process is fundamental to the mechanism by which Cu(II) thiosemicarbazone complexes (e.g., Cu-ATSM) accumulate in hypoxic tissue.[6,7] Additionally, bioreduction may be responsible for the loss of radioactive copper from other ligand systems.[8,9]

To overcome instability issues, ligands that form ^{64}Cu(II) complexes with high thermodynamic stability and kinetic inertness are required. Hexaazamacrobicyclic cage ligands (sarcophagines) are a promising ligand class for ^{64}Cu(II)-based imaging applications. For example, the Cu(II) complex of $(NH_2)_2$Sar (**1**, Figure 1), displays very high thermodynamic stability and, because of encapsulation of the metal ion in the cage ligand, is inert to metal dissociation.[1] In early studies, a $(NH_2)_2$Sar derivative - SarAr (**2**, Figure 1) was developed to allow the efficient bioconjugation of sarcophagine ligands, and ^{64}Cu-**2** monoclonal antibody (mAb) immunoconjugates were used for PET imaging of neuroblastoma and melanoma xenografts in mice.[10−12] More recently, Donnelly and coworkers have introduced a pendent carboxylate functional group to $(NH_2)_2$Sar, yielding Sar-CO_2H (**3**, Figure 1), via a ring-opening reaction between $[Cu(II)(NH_2)_2Sar]^{2+}$ and glycolic anhydride.[13] The ^{64}Cu-**3**-rituximab immunobioconjugate was prepared, and this compound showed good in vivo plasma stability.[14]

Received: September 26, 2013
Published: December 16, 2013

   dx.doi.org/10.1021/ic4024508 | *Inorg. Chem.* 2014, 53, 468−477

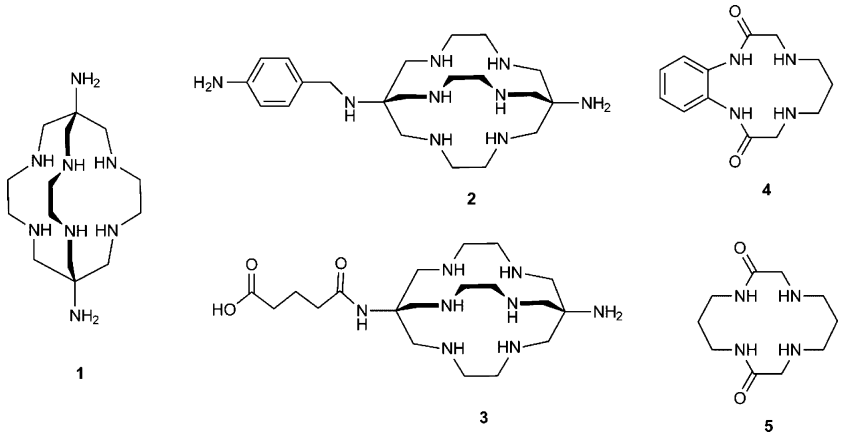

Figure 1. Structures of macrobicyclic chelators (**1**–**3**) and diamide/diamine tetraaza-macrocycles (**4** and **5**) used to form complexes with copper-64.

Deprotonated amide (amidate or amido) groups are strong σ-donors and are well-known to stabilize metal ions in higher oxidation states. Margerum and co-workers conducted ground breaking early studies on this phenomenon and showed that Cu(II) and Ni(II) complexes of peptides could be readily oxidized to their Cu(III) and Ni(III) counterparts.[15−18] More recently, Collins and co-workers have developed a range of acyclic and macrocyclic amide containing ligands for the stabilization of high oxidation state metal centers for use as green oxidation catalysts.[19−23] Amido donors have also been successfully utilized in radiopharmaceutical development. For example, ^{99m}Tc-Depreotide (Neotect), a clinical radiopharmaceutical used for imaging somatostatin receptor positive tumors,[24] displays N_3S chelation, consisting of amido (2), thiolate, and amine donor groups.[25] The related ligand system, mercaptoacetyltriglycine (MAG3) in combination with ^{99m}Tc, is an approved radiopharmaceutical used for the evaluation of renal transplant blood flow and function.[26]

The synthesis and ^{64}Cu radiolabeling studies of the diamidediamine macrocycle **4** (Figure 1) has been reported.[27,28] The Cu(II) complex of this ligand has a highly negative reduction potential (−1.84 V vs SCE) and as such is expected to be resistant to reduction in vivo, and biodistribution studies for the ^{64}Cu labeled complex showed rapid clearance of radioactivity from the blood suggesting good complex stability. A series of six aliphatic diamidediamine macrocycles with different chelate ring sizes (e.g., **5**, Figure 1) have been radiolabeled with ^{64}Cu.[29] These studies showed significant variation in the labeling efficiency for the different macrocycles, and only ligand **5** readily formed a ^{64}Cu complex with high purity. Biodistribution studies for this complex showed rapid blood, liver and kidney clearance.[29]

We herein report the synthesis of two novel triamidetriamine cryptand ligands, which differ in their molecular architecture, with one being macrobicyclic and the other macrotricyclic. The Co(III) and Cu(II) complexes of the macrobicyclic ligand have been prepared and the Co(III) complex displays octahedral coordination with three amine and three deprotonated amido nitrogen atoms coordinated to the metal atom. In contrast, the Cu(II) center is not encapsulated by the ligand but rather adopts a square planar coordination geometry, with two amine and two deprotonated amido donor groups. Electrochemical and spectroelectrochemical studies were conducted to gain insight into the oxidative stability of the Cu(II) complex. Copper-64 radiolabeling was carried out for the macrobicyclic ligand, and the complex showed no evidence of instability when subjected to ligand challenge experiments with the metal binding amino acid L-cysteine, however, incubation with L-histidine resulted in low levels of decomplexation.

RESULTS AND DISCUSSION

Synthesis. The triamidetriamine cryptand ligands (**7** and **8**) were prepared by the reaction of the tripodal α-chloroamide precursor (**6**) with either 1,1,1-*tris*(aminoethyl)ethane (tame) or 1,4,7-triazacyclononane (tacn) respectively. The *tris*(α-chloroamide) synthetic intermediate (**6**) was synthesized by treating tame with 3 equiv of 2-chloroacetyl chloride (Scheme 1). As expected, the C_3 symmetric molecule gave rise to simple ^{1}H and ^{13}C NMR spectra with a broad triplet signal at 7.78 ppm observed for the amide N−H groups. Cryptands **7** and **8** were prepared from equimolar mixtures of **6** and the triamines: tame or tacn respectively and the mild base K_2CO_3 (Scheme 1). The reactions were carried out under high dilution in refluxing acetonitrile, in an effort to improve the yield of the cryptand products. In both cases, relatively long reaction times were

Scheme 1. Synthesis of the *tris*(α-Chloroamide) Precursor 6 and the Cryptands 7 and 8 Utilizing 6 and the Triamines 1,1,1-*tris*(Aminoethyl)ethane (tame) or 1,4,7-Triazacyclononane (tacn) (S3 and S6 Respectively, Supporting Information)

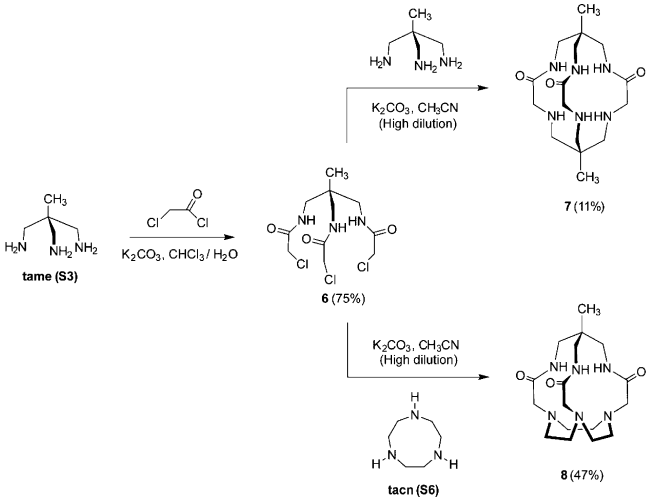

dx.doi.org/10.1021/ic4024508 | Inorg. Chem. 2014, 53, 468−477

used, as over the course of several experiments it became apparent that increased reaction times lead to improved product yields. Markedly different yields (11% and 47% respectively) were obtained for cryptands **7** and **8**, and this difference appears to be the result of the different levels of conformational freedom associated with the triamines: tame and tacn. Here, the acyclic tame molecule in conjunction with the highly flexible α-chloroamide precursor (**6**) results in a poor yield of the desired macrobicycle **7**, while the lower level of conformational freedom associated with the cyclic tacn molecule leads to an improved yield of the macrotricycle **8**. Attempts were made to increase product yields by the introduction of a halide anion, for example, Cl^- or Br^- (as the Bu_4N^+ salts), as a templating agent for the α-chloroamide precursor (**6**) (via hydrogen bonding with amide N−H groups). However, this variation in the synthetic procedure resulted in much poorer yields of the desired products, with unidentified byproducts being generated.

The number of signals observed in the ^{1}H and ^{13}C NMR spectra for **7** and **8** (Figures S2 and S3, Supporting Information) are consistent with these cryptands exhibiting C_3 (point group C_{3v}) symmetry in solution. The amine and amide N−H protons of **7** resonate as broad singlet and triplet signals at 1.86 ppm and 7.21 ppm respectively, while for **8** the amide N−H protons resonate as a broad triplet signal at 7.92 ppm. For the macrotricycle **8** the six methylene units of the triazacyclononane molecular component are equivalent, giving rise to a single ^{13}C signal at 53.5 ppm. In contrast, the methylene proton environments of this molecular fragment (H7a and H7b, Supporting Information) are inequivalent, with one proton being "endo" and the other "exo" with respect to the macrocycle, and these protons resonate as a relatively complex AA′BB′ pattern.

With the cryptands (**7** and **8**) on hand, we initially focused on synthesizing the Co(III) complexes of these ligands. Cobalt(III) was chosen as this cation has previously been used to form neutral, octahedral complexes with two tripodal, triamide ligands, where the amide N−H groups were deprotonated and coordinated to the metal center.[30] The Co(III) complex **9** was prepared by aerating an aqueous mixture of **7** and $CoCl_2$ for three days (Scheme 2). The neutral complex was separated from charged species by passage through both cation and anion (CM- and DEAE-Sephadex) exchange resins. Despite several attempts, the Co(III) complex of cryptand **8** could not be synthesized. Because of our interest in the development of these cryptand ligands for radiopharmaceutical applications, we also investigated the chemistry of **7** and **8** with Cu(II). The Cu(II) complex **10**, was prepared by adding 3 equiv of NaOH to an equimolar aqueous mixture of **7** and $CuCl_2$ (Scheme 2). As was the case with Co(III), the Cu(II) complex of **8** could not be prepared.

Scheme 2. Synthesis of Co(III) (9) and Cu(II) (10) Complexes of Cryptand 7

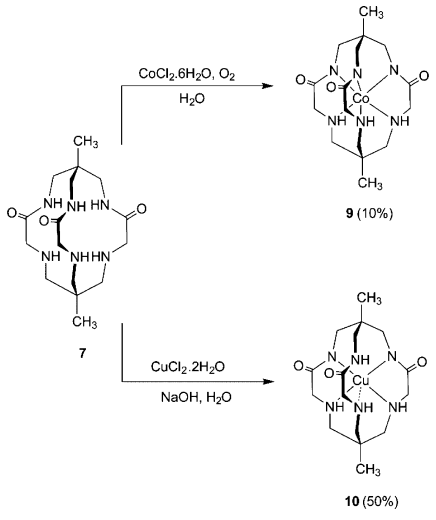

The ^{1}H NMR and ^{13}C NMR spectra of **9** are consistent with the Co(III) complex possessing C_3 symmetry. The ^{1}H NMR spectrum is characterized by two singlet signals for the inequivalent methyl groups, while the methylene groups of the magnetically equivalent "straps" of the macrobicycle give rise to three sets of AB doublet pairs. The AB patterns are consistent with C_3 symmetry as opposed to the C_{3v} symmetry of the ligand. In interpreting these spectra, it is useful to consider the hexaaminemacrobicyclic cage family of ligands developed by Sargeson and co-workers. As an example, the ^{1}H NMR spectrum of $[Co(III)(sepulcrate)]^{3+}$ (**11**, Figure 2), shows AB doublet pairs for the cap methylene groups and more complex A_2B_2 patterns for the ethylenediamine protons.[31]

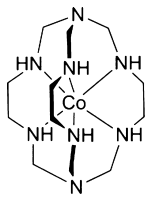

11

Figure 2. Structure of $[Co(III)(sepulcrate)]^{3+}$ (**11**).[31]

Here the right- or left-handed "twist" (Δ or Λ) induced in the sepulcrate by the octahedral coordination geometry of the metal, leads to inequivalent environments for the methylene group protons and defines the configuration (R or S) for the six coordinated amine groups.[31] Similarly for **9**, (as confirmed by the X-ray crystallographic structural studies, vide infra), the octahedral complex is formed as a racemic mixture of Δ and Λ stereoisomers, and the "twist" in ligand coordination geometry results in inequivalent proton environments for the methylene group protons.

Based on the structure of previously reported Cu(II) complexes of hexaaminemacrobicyclic cage ligands, for example, **2**,[32] it was anticipated that the cryptate ligand **7** may form an anionic, tetragonally distorted octahedral Cu(II) complex, with all three amide N−H groups deprotonated and coordinated to the metal center. No evidence of an anionic complex could be detected in the negative ion ESI-MS spectrum of **10**, indicating that Cu(II) does not form a complex involving deprotonation of all three amide groups of the ligand. The base peak in the positive ion ESI-MS spectrum of **10** (Supporting Information, Figure S4) is consistent with the formula $[C_{16}H_{29}CuN_6O_3]^+$. Here two amide groups are deprotonated and coordinated to the Cu(II) center but the third remains protonated and likely does not bind to the metal. Consistent with this result, the most likely coordination geometry is square-planar, where two of the secondary amine groups also bind to the metal and the third amine is protonated

dx.doi.org/10.1021/ic4024508 | Inorg. Chem. 2014, 53, 468−477

yielding an ammonium group and the overall cationic charge on the molecule.

The electronic absorption spectrum of **10** (Figure 3) was recorded to further probe the coordination mode of this Cu(II)

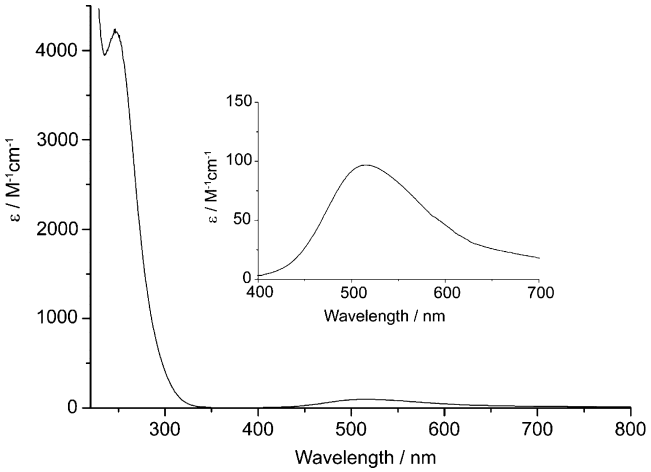

Figure 3. Ultraviolet−visible spectrum of an aqueous solution of **10** (1.0×10^{-3} M).

complex. The spectrum is characterized by a moderately intense absorption band centered at 248 nm (ε = 4207 M^{-1} cm^{-1}) and a broad, weak band centered at 516 nm (ε = 97 M^{-1} cm^{-1}). The electronic absorption spectrum of **10** closely resembles those of a number of square-planar Cu(II) complexes of diamidediamine macrocycles, for example, **4** and **5**.[28,33] In particular, these square-planar complexes consistently display a weak band in the visible region (~500 nm, ε = ~100 M^{-1} cm^{-1}). Density functional theory (DFT) calculations for the Cu(II) complex of **4** indicate that this weak absorption band results from the redistribution of electron density between metal centered d orbitals.[28] Based on the mass spectrometric and electronic absorption results, it appears likely that the Jahn−Teller distortion associated with the d^9 electron configuration of Cu(II) causes the metal to adopt a square-planar coordination geometry, with two amido and two amine donors.

To investigate differences in the interaction of cryptands **7** and **8** with $CuCl_2$, equimolar aqueous solutions of the chosen cryptand and $CuCl_2$ were mixed and UV−visible spectra were recorded at 5 and 60 min after mixing. The spectra (Figures S5 and S6 respectively, Supporting Information) show that Cu^{2+} complexation by cryptand **7** was rapid with the 248 and 516 nm absorption bands evident at 5 min. Absorption bands arising at ~250 nm have been previously assigned to a charge-transfer transition associated with Cu^{2+} coordinated to deprotonated amide nitrogen atoms.[34] In contrast the only change observed for cryptand **8** after mixing was a red shift in the high energy n→π^* transition of the ligand amide group, which is likely to be associated with a weak interaction between the metal and the carbonyl oxygen. These results support the notion that for cryptand **8**, Cu^{2+}-amine coordination does not occur and as a result amide group deprotonation and coordination is unfavorable. In comparison to **7**, ligand **8** is a relatively rigid

Table 1. Crystal Refinement Data

	6	7	8	9	10
empirical formula	$C_{11}H_{18}N_3O_3Cl_3$	$C_{16}H_{30}N_6O_3$	$C_{17}H_{30}N_6O_3$	$C_{17.5}$ $H_{33}CoN_6O_{4.5}$	$C_{17}H_{32}CuN_6O_4$
formula weight	346.63	354.46	366.47	458.43	448.03
temperature/K	173	173	173	173	173
crystal system	monoclinic	monoclinic	monoclinic	monoclinic	monoclinic
space group	*Pc*	$P2_1/c$	$P2_1/c$	$P2_1/n$	$P2_1/c$
a/Å	7.9147(2)	15.9861(2)	10.337(2)	15.7221(7)	11.2087(6)
b/Å	11.1818(2)	14.9331(2)	15.943(3)	7.8240(3)	8.4478(5)
c/Å	9.5726(3)	15.0549(2)	10.759(2)	17.6366(7)	22.7388(11)
β/deg	113.626(3)	97.8150(10)	94.84(3)	106.127(4)	114.940(4)
volume/Å^3	776.17(3)	3560.56(8)	1766.9(6)	2084.10(15)	1952.33(18)
Z	2	8	4	4	4
ρ(calc) mg/mm^3	1.483	1.322	1.378	1.461	1.524
μ/mm^{-1}	5.45	0.766	0.097	0.863	1.156
Crystal size/mm^3	0.15 × 0.12 × 0.1	0.15 × 0.08 × 0.02	0.12 × 0.12 × 0.05	0.15 × 0.1 × 0.1	0.3 × 0.12 × 0.03
wavelength/Å	Cu−Kα 1.54184	Cu−Kα 1.54184	Mo−Kα 0.71073	Mo−Kα 0.71073	Mo−Kα 0.71073
2θ range for data collection	7.9 to 130.04°	5.58 to 147.84°	5.838 to 54.204°	4.8 to 58.8°	6.04 to 52.74°
index ranges	$-6 \le h \le 9$	$-19 \le h \le 19$	$-13 \le h \le 13$	$-18 \le h \le 20$	$-9 \le h \le 14$
	$-11 \le k \le 13$	$-18 \le k \le 16$	$-20 \le k \le 20$	$-6 \le k \le 10$	$-10 \le k \le 10$
	$-11 \le l \le 11$	$-17 \le l \le 18$	$-13 \le l \le 13$	$-22 \le l \le 24$	$-28 \le l \le 28$
reflections collected	2449	14408	30912	12100	12047
independent reflections	1604 [*R*(int) = 0.0202]	7014 [*R*(int) = 0.0255]	3896 [*R*(int) = 0.0262]	4966 [*R*(int) = 0.039]	3993 [*R*(int) = 0.0341]
data/restraints/parameters	1604/2/182	7014/7/479	3896/0/236	4966/1/274	3993/2/261
goodness-of-fit on F^2	1.1	0.861	1.046	1.023	1.042
final *R* indexes [$I \ge 2\sigma$ (*I*)]	R_1 = 0.0400	R_1 = 0.0413	R_1 = 0.0352	R_1 = 0.0471	R_1 = 0.0368
	wR_2 = 0.1014	wR_2 = 0.1136	wR_2 = 0.0873	wR_2 = 0.1010	wR_2 = 0.0886
final *R* indexes [all data]	R_1 = 0.0401	R_1 = 0.0518	R_1 = 0.0403	R_1 = 0.0783	R_1 = 0.0467
	wR_2 = 0.1018	wR_2 = 0.1250	wR_2 = 0.0908	wR_2 = 0.1161	wR_2 = 0.0936
largest diff. peak/hole/e Å^{-3}	0.37/−0.42	0.32/−0.28	0.31/−0.23	0.60/−0.47	0.93/−0.52
Flack parameter	0.017(19)				

dx.doi.org/10.1021/ic4024508 | *Inorg. Chem.* 2014, 53, 468−477

Table 2. Selected Bond Distances (Å) from the X-ray Crystal Structures of 6−10

	6	7	8	9 (M = Co(III))	10 (M =Cu(II))
N2A−C3A	1.338(5)	1.347(2)	1.342(2)	1.308(3)	1.342(3)
N2B−C3B	1.318(5)	1.328(2)	1.335(2)	1.306(3)	1.309(3)
N2C−C3C	1.330(5)	1.355(2)	1.342(2)	1.315(4)	1.318(3)
N2A−M				1.890(2)	
N2B−M				1.900(2)	1.928(2)
N2C−M				1.898(2)	1.934(2)
N5A−M				1.965(2)	2.403(2)
N5B−M				1.967(2)	2.028(2)
N5C−M				1.954(2)	2.003(2)

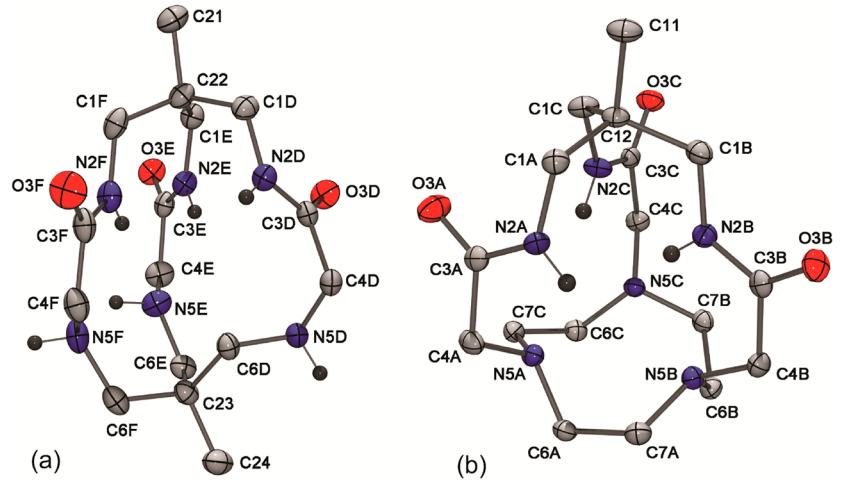

Figure 4. ORTEP[35] structures of (a) 7 (Z' = 2, the second conformational isomeric form of the cryptand has been omitted for clarity) and (b) 8 (N−H hydrogen atoms shown). Thermal ellipsoids are shown at 50% probability levels.

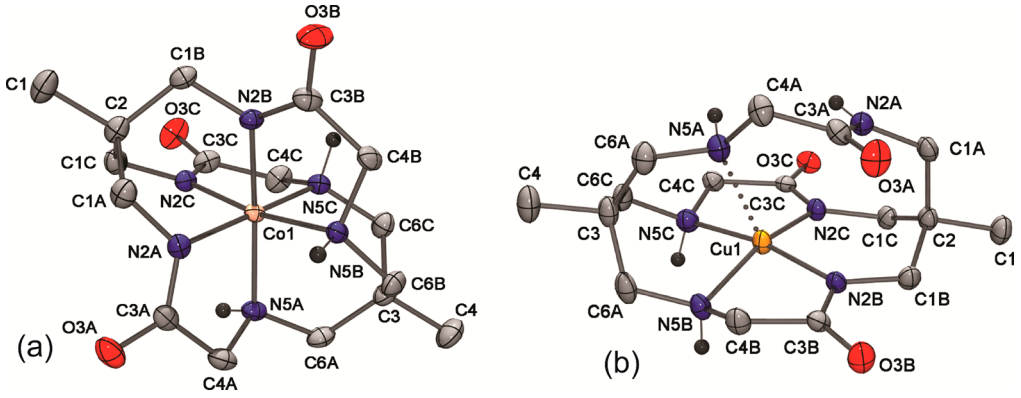

Figure 5. ORTEP[35] structures of (a) 9 (two cocrystallized methanol molecules omitted for clarity) and (b) 10 (one cocrystallized methanol molecule omitted for clarity) (N−H hydrogen atoms shown). Thermal ellipsoids are shown at 50% probability levels.

molecule, and the X-ray structure (vide infra) shows that the amine lone pairs are endocyclic (endohedral) and may not be accessible to the metal center.

Structural Studies. The crystal structures of compounds **6**−**10** were determined, and the crystallographic refinement data are given in Table 1 and selected bond distances in Table 2. The tripodal precursor **6** crystallized in the chiral space group *Pc* and the structure of this compound is shown in Figure S7 (Supporting Information). Although compound **6** is achiral, the conformational isomeric form of **6** found in the solid state is chiral. The structure of **6** is strongly influenced by amide group N−H···O hydrogen bonding, with both intra- (N2A−O3B = 2.942(4) Å and N2C−O3A = 3.000(6) Å) and intermolecular (N2B−O3B = 2.869(5) Å, symmetry operator x, $1-y$, $1/2+z$) hydrogen bonds present. The cryptands **7** and **8** both crystallize in the monoclinic space group $P2_1/c$, and the structures of these molecules are shown in Figure 4, panels a and b, respectively. In the case of **7**, two independent conformational isomeric forms of the cryptand are present in the asymmetric unit. As expected, all amide groups for **7** and **8** adopt the trans configuration, and extensive amide and amine group hydrogen bonding interactions are present.

The Co(III) complex, **9** crystallizes in the monoclinic space group $P2_1/n$, and the structure is shown in Figure 5a. The Co(III) center sits in a relatively undistorted octahedral coordination geometry with three facial sites occupied by the

dx.doi.org/10.1021/ic4024508 | Inorg. Chem. 2014, 53, 468−477

deprotonated amido nitrogen atoms and the other three by the amine nitrogen atoms. The complex possesses four chiral centers, these being the Co(III) center (Δ and Λ) and the three coordinated amine groups (R and S). The chirality of the amine groups is defined by the Co(III) center, where if Co(III) = Δ the coordinated amine groups adopt an S configuration (alternatively, Co(III) = Λ, amine = R). The three five-membered chelate rings are nonplanar and adopt an *ob* (obverse) conformation with respect to the C_3 axis through the metal center, yielding an overall ob_3 molecular configuration. The ob_3 configuration is the same as that reported previously for the Co(III) complex of an acyclic tripodal, triamidetriamine ligand [Co(2,2′,2″-trioxosen-3*H*)].[30] The average of the Co−N_{amido} distances (1.896(2) Å) is significantly shorter than that of the Co−N_{amine} bond lengths (1.962(2) Å). This difference is expected, as anionic amido groups are strong σ-donors and exert a marked trans-influence, leading to a lengthening of the Co−N_{amine} bonds. Interestingly the Co−N_{amine} bond lengths for **9** are shorter than those reported previously for [Co(2,2′,2″-trioxosen-3*H*)], where the average of the three Co−N_{amine} bond lengths was 1.996(4) Å.[30] This shortening of the Co−N_{amine} distances most likely arises as a result of the constraints imposed on these bonds by the relatively inflexible macrobicyclic ligand. Such a notion is supported by comparison to structurally related Co(III) complexes of hexaaminemacrobicyclic cage complexes, for example, the average of the Co−N_{amine} bond lengths for $[Co\{(NMe_3)_2\text{-Sar}\}]^{5+}$ was 1.961(6) Å.[36] To the best of our knowledge there is only one other example of an amide bearing sarcophagine cryptand and for the Co(III) complex of this monoamide molecule, $[Co(III)(Me,CO_2H\text{-oxosar}-H]^{2+}$, the Co−$N_{amido}$ distance was 1.917(4) Å.[37]

The Cu(II) complex, **10** crystallizes in the monoclinic space group $P2_1/c$, and the structure is shown in Figure 5b. The X-ray structure confirms the results of the mass spectrometric and UV−visible studies and shows that the Cu(II) center sits in a distorted square planar geometry, with coordination from two deprotonated amido nitrogen atoms and two amine nitrogen donors. As was the case for the Co(III) complex **9**, the average of the Cu−N_{amido} distances (1.931(2) Å) is significantly less than that of the Cu−N_{amine} bond lengths (2.016(2) Å). Similar or slightly shorter distances have been reported previously for two related square planar Cu(II) complexes of aliphatic diamidediamine macrocyclic ligands, these being 1.948(2) Å and 2.019(2) Å[38] and 1.887(3) Å and 1.991(2) Å[39] for the Cu−N_{amido} and Cu−N_{amine} bond lengths, respectively. Examination of the structure shows a weak axial interaction between the Cu(II) atom and the third amine group of the macrobicyclic molecule, with this Cu−N_{amine} distance being 2.403(2) Å. The square-planar coordination geometry is distorted with the Cu(II) center being displaced above the least-squares plane defined by the four nitrogen atoms (N2B, N2C, N5B, and N5C) by 0.261(1) Å toward the third axial amine group. The two amine nitrogen atoms coordinated to the Cu(II) center (N5B and N5C) are chiral with one of these groups adopting an R and the other an S configuration, and as such **10** can be described as a meso compound.

Electrochemistry and Spectroelectrochemistry. The electrochemical properties of **10** were studied using cyclic voltammetry, and Figure 6a shows the cyclic voltammetric response for an aqueous solution of **10** (1 mM) containing 0.1 M $LiClO_4$ as supporting electrolyte. When scanned anodically, the complex exhibits a one-electron oxidation process centered at 0.75 V vs Ag/AgCl, which can be assigned to the $Cu^{2+/3+}$ redox couple. The redox couple is electrochemically and chemically quasi-reversible at scan rates of approximately 0.2 V s^{-1} and above, with the ratio of oxidative and reductive peak currents ($i_{p,ox}/i_{p,red}$) being close to unity and the peak-to-peak splitting (ΔE_p) being 90 mV at 0.2 V s^{-1}. However the response becomes progressively less chemically reversible as the scan rate is decreased, until the return wave disappears entirely at about 0.01 V s^{-1}. These observations are consistent with an EC type mechanism where the complex undergoes a chemical transformation on oxidation. That this homogeneous reaction can be out-run at moderate voltammetric time scales suggests that the kinetics for this process are relatively slow.

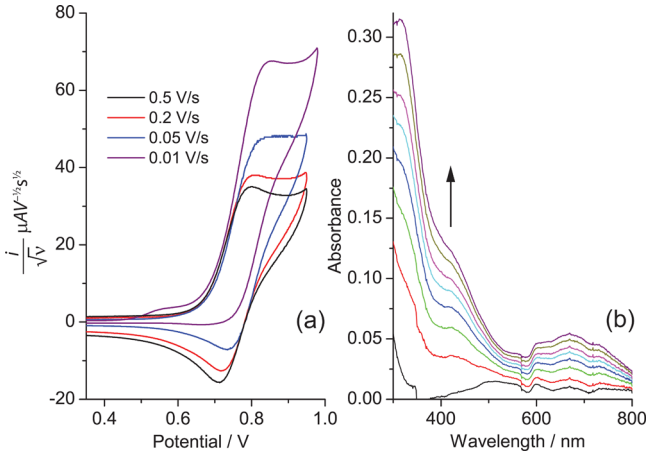

Figure 6. (a) Cyclic voltammetric responses at varying scan rate for a 1.0 mM aqueous solution of **10** containing 0.1 M $LiClO_4$ as supporting electrolyte. The current axis has been normalized by a factor of $\nu^{-1/2}$ (where ν is scan rate) to highlight kinetic effects. (b) Changes in the UV−visible absorbance spectrum during electrolysis of 1.0 mM solution of **10** in water containing 0.1 M $LiClO_4$ as supporting electrolyte. The potential of the platinum gauze working electrode was held at a constant value of 1.0 V vs Ag/AgCl during the course of the oxidation.

To probe the nature of the oxidized species, spectroelectrochemical measurements were performed, and the changes in the visible absorption spectrum while electrochemically oxidizing a 1.0 mM solution of **10** are shown in Figure 6b. The potential was maintained at 1.0 V versus the Ag/AgCl reference electrode, and a spectrum acquired every 10 s until no further spectroscopic changes were observed. A general increase in absorption is observed with an oxidizing potential applied, with new absorbance bands appearing at ∼320 and 415 nm accompanied by a visual color change from pale purple to green. Such changes are consistent with those observed previously for Cu(III) complexes of ligands bearing deprotonated amide donors, for example, biuret,[40] tetraglycine,[41] and the diamide macrocycle **4**.[28] The observed spectral changes due to the oxidative process are only partially reversible, and the spectrum for the original Cu(II) complex was not fully regenerated through bulk electrolysis when a potential more negative than the oxidation peak was applied (results not shown). This is consistent with the voltammetric response presented in Figure 6a, which is also irreversible at long experimental time scales (slow scan rates). The absence of an isosbestic point also supports the notion of an EC type mechanism accompanying the oxidation process.

Copper-64 Labeling Studies. Cryptand **7** was radiolabeled with $^{64}Cu(II)$ by heating a solution of **7** (0.1 mg) and $^{64}CuCl_2$ (23.1 MBq) at 86 °C for 1 h in ammonium acetate

dx.doi.org/10.1021/ic4024508 | *Inorg. Chem.* 2014, 53, 468−477

buffer (0.4 M, pH 5.5) to give ^{64}Cu-**10** in a decay corrected yield of 75.7% after HPLC isolation and mobile phase evaporation, which took 93 min including the 1 h reaction time. The yield based on integration of the activity channel chromatogram was somewhat higher indicating that 84% of the radioactivity was associated with the ^{64}Cu-**10** peak; this discrepancy is understandable on account of the losses associated with collection of the radiolabeled compound and geometric and attenuation considerations in the dose calibrator. The identity of the peak was confirmed by coinjection of a ^{64}Cu-**10** and Cu-**10** mixture (Figure 7), where the peak maxima

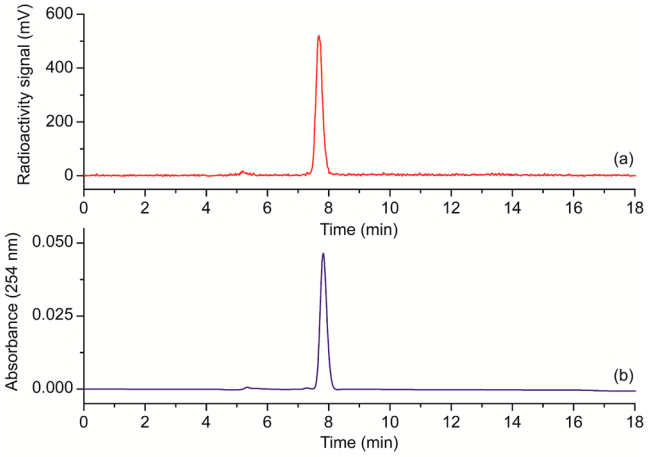

Figure 7. Radioactivity (a) and absorbance (254 nm) (b) HPLC chromatograms obtained from the coinjection of a mixture of ^{64}Cu-**10** and Cu-**10**. The peak maxima for the radioactivity channel and the 254 nm absorbance channel are coincident (allowing for the arrangement of the radioactivity and UV detection systems).

of the radioactivity channel and the 254 nm absorbance coincided. Earlier attempts to label **7** with ^{64}Cu were unsuccessful on account of trace impurities in the ligand, prior to HPLC purification. To evaluate the stability of ^{64}Cu-**10**, ligand challenge experiments were conducted using the well-known metal binding amino acids: L-histidine and L-cysteine. For these experiments, samples of ^{64}Cu-**10** (~1.3 MBq) reconstituted in phosphate buffered saline (PBS) pH = 7.4, were incubated at 37 °C for 24 h with either no addition (control) or with L-cysteine or L-histidine (1×10^{-3} M). Radio-HPLC analysis Figures S8–S10 (Supporting Information) showed evidence for trans-chelation in the presence of L-histidine over the course of the experiment with the radiochemical purity being 93% and 70.2% after 6 and 24 h respectively. The L-cysteine challenge on the other hand resulted in ^{64}Cu-**10** of a radiochemical purity of greater than 98% after the 24 h period, which was very similar to the PBS control. These results show that ^{64}Cu-**10** displays good stability in the presence of very high concentrations of competing ligands and that trans-chelation of ^{64}Cu is more facile in the presence of N-donor amino acid, L-histidine.

CONCLUSION

The first examples of triamidetriamine cryptand ligands (**7** and **8**) were successfully prepared from the *tris*(*α*-chloroamide) synthetic intermediate **6** and the triamines: tame or tacn, respectively. Encapsulating ligands are of significant current interest for radiopharmaceutical applications utilizing ^{64}Cu,[10−14,42] and the simple yet versatile synthetic approach described here represents a novel strategy for the synthesis of cage ligands. Previous attempts to prepare triamidetriamine cryptands by capping the acyclic [Co(2,2′,2″-trioxosen-3*H*)] precursor with methanal and nitromethane were unsuccessful, presumably because of the electronic influence of the deprotonated amido groups.[30] A diamide containing sarcophagine has been proposed as a reaction intermediate formed from 3,6,10,13,16,19-hexaazabicyclo[6.6.6]eicosane and dimethyloxalate; however, this compound was not isolated.[43] Cryptand **7** was metalated with Co(III) or Cu(II). In contrast, and despite numerous attempts, cryptand **8** could not be metalated with these metal ions. The low metal-binding affinity of **8** was unexpected as tacn and tacn based ligands generally bind as facial tridentates, and visual examination of the crystal structure of **8** suggests a significant degree of preorganization of the tacn molecular component for metalation as a facial tridentate. In addition, the structurally related complex [Co(III)(nosartacn)]$^{3+}$ (**12**, Figure 8) of a hexaaminemacro-

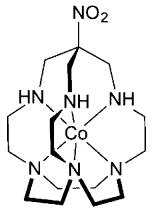

12

Figure 8. Structure of [Co(III)(nosartacn)]$^{3+}$ (**12**).[44]

tricyclic ligand has been reported previously.[44] In contrast to the present work however, **12** was prepared by capping the trigonal face of the precursor complex [Co(taetacn)]$^{3+}$, as opposed to direct metalation of the free cryptand ligand.[44]

A possible explanation for our inability to metalate **8** may be associated with the lower flexibility of this ligand because of the introduction of the third macrocyclic ring. This change is likely to lower the conformational freedom of **8** when compared to **7** and may decrease the capacity of the ligand to accommodate an octahedral metal ion and instead impose the less favorable trigonal prismatic coordination geometry. Additionally, the X-ray structure of **8** shows that the amine nitrogen atom lone pairs are endocyclic (endohedral) and may not be accessible to the metal center.

The X-ray crystal structure for the Co(III) complex **9** support the results of the ^{1}H and ^{13}C NMR studies, which show that the complex possesses C_3 symmetry. The structure of this complex is closely related to those of Sargeson's hexaaminemacrobicyclic cage family of ligands, with the three five-membered chelate rings adopting an *ob* conformation with respect to the C_3 axis. Similarly the X-ray crystal structure of the Cu(II) complex **10** confirms the results of the mass spectrometric and UV–visible studies and shows that the deprotonated amido nitrogen donors favor a tetragonally distorted square-planar coordination geometry for the Cu(II) center.

Cyclic voltammetric studies of **10** show an oxidative response with E° = 0.75 V (versus Ag/AgCl). This process is reversible at most scan rates but becomes irreversible at scan rates of about 0.01 V s^{-1}, suggesting a kinetically slow chemical reaction following oxidation. Spectroelectrochemical experiments con-

dx.doi.org/10.1021/ic4024508 | *Inorg. Chem.* 2014, 53, 468–477

firm the formation of a new product when electrolysis is carried out for relatively long periods of time. Although the nature of the decomposition product formed on oxidation is unknown, the results are consistent with a scenario where the metal center withdraws electron density from one of the metal ligand bonds on oxidation, resulting in cleavage of that bond and formation of an aquo complex. Because of our interest in the development of these cryptand ligands for radiopharmaceutical applications, ligand **7** was radiolabeled with ^{64}Cu. Although, the ^{64}Cu(II) ion was not encapsulated by **7** in a manner analogous to hexaamine sarcophagine ligands,[32,45] ^{64}Cu-**10** showed no evidence of decomposition when incubated with the amino acid L-cysteine and moderate levels of ^{64}Cu transchelation in the presence of the N-donating L-histidine. We are currently investigating the chemistry of cryptand **7** with Ga(III) as ^{68}Ga has excellent properties for PET imaging (β^+ = 89%, $E_{\beta^+\,max}$ = 1.92 MeV, $t_{1/2}$ = 68 min), and the results of these studies will be reported in due course.

EXPERIMENTAL SECTION

General Procedures. Unless otherwise stated, all manipulations were performed under a nitrogen atmosphere. All chemicals and reagents were purchased from commercial sources (Sigma Aldrich or Alfa Aesar) and were of analytical grade or higher, and were used as received. Anhydrous tetrahydrofuran was distilled from potassium under nitrogen prior to use. Anhydrous acetonitrile was distilled from CaH_2 under nitrogen, and stored over molecular sieves (4 Å, activated at 250 °C) prior to use. Potassium carbonate was dried in a furnace at 200 °C for 12 h prior to use. NMR spectra were recorded on a Bruker Avance ARX-300 (300.14 MHz for ^{1}H, 75.48 MHz for ^{13}C) and Bruker Avance ARX-500 (500.13 MHz for ^{1}H, 125.77 MHz for ^{13}C) spectrometer and were internally referenced to solvent resonances. Mass spectra were obtained using a Bruker Esquire6000 mass spectrometer fitted with an Agilent electrospray (ESI) ion source. UV−visible spectra were recorded using an Agilent Technologies Cary 300 UV−visible spectrophotometer using quartz cuvettes (1 cm). The triamines tame[46−48] and tacn[49,50] were prepared using modified literature procedures (Supporting Information). The compound numbering scheme used for ^{1}H and ^{13}C NMR assignments are given in the Supporting Information.

X-ray Crystallography. Single crystals suitable for X-ray crystallography were grown as follows: the diffusion of vapors between hexane and a chloroform solution of the title compound (**6**); the diffusion of vapors between diethyl ether and chloroform solutions of the title compounds (**7** and **8**) or methanol solutions of the title compounds (**9** and **10**). Crystallographic data for all structures determined are given in Tables 1 and 2. For all samples, crystals were removed from the crystallization vial and immediately coated with Paratone oil on a glass slide. A suitable crystal was mounted in Paratone oil on a glass fiber and cooled rapidly to 173 K in a stream of cold N_2 using an Oxford Instruments low temperature device. Diffraction data were measured using an Oxford Gemini diffractometer mounted with Mo−Kα (λ = 0.71073 Å) or Cu−Kα (λ = 1.54184 Å) radiation. Data were reduced and corrected for absorption using the CrysAlis Pro program.[51] The structures were solved using Direct Methods and refined by the Full-Matrix Least-Squares refinement techniques on F^2 using SHELXL97.[52] The non-hydrogen atoms were refined anisotropically and hydrogen atoms were placed geometrically and refined using the riding model. Coordinates and anisotropic thermal parameters of all non-hydrogen atoms were refined. All calculations were carried out using the program Olex^2.[53] Images were generated by using ORTEP-3.[35] Further X-ray diffraction (XRD) details are provided in the Supporting Information. CCDC 961215−961219 contains the supplementary crystallographic data for this paper. These data can be obtained free of charge from The Cambridge Crystallographic Data Centre via www.ccdc.cam.ac.uk/data_request/cif

Electrochemical and Spectroelectrochemical Studies. All electrochemical experiments were conducted at room temperature in aqueous 0.1 M $LiClO_4$ which was purged with argon prior to experiments. Cyclic voltammetry was performed using a CHI660E potentiostat (CH Instruments, Austin, TX, U.S.A.). The electrochemical cell was a conventional three-electrode configuration, consisting of a glassy carbon 3 mm (0.07068 cm^2) working electrode shrouded in Teflon (CH Instruments), a 1 cm^2 platinum gauze auxiliary electrode, and an aqueous Ag/AgCl (3 M KCl) reference electrode (CH Instruments). Spectro-electrochemical measurements were performed using a Varian Cary UV−visible spectrometer and a CH660B potentiostat (CH Instruments) with a 1 mm path length thin layer quartz spectroelectrochemical cell (ALS, Tokyo, Japan). A fine platinum gauze working electrode, platinum wire counter electrode, and Ag/AgCl (3 M KCl) reference electrode were employed.

Radiochemistry. All radiochemistry reactions involving ^{64}Cu were carried out in suitably lead shielded fume hoods in plastic-ware that had been soaked in 4 M HCl overnight followed by washing with deionized H_2O (18.2 MΩ) and drying. Radioactivity measurements were performed on a CAPINTEC CRC-15R Dose Calibrator with calibration factor set to #035. Purification of the ^{64}Cu-**10** radiocomplex was performed on a Waters Empower^2 controlled HPLC with a Waters 600E pump, a Rheodyne manual injection port, Waters 2998 Photodiode Array, and a Carroll & Ramsay Associates 105S γ-detector with a sodium iodide crystal. Stability analysis of the ^{64}Cu-**10** radiocomplex was performed on a Waters Empower^2 controlled HPLC with a Waters 600E pump, a Rheodyne manual injection port, a Waters 2489 Dual channel UV/visible detector, and a LabLogic IN/US Systems γ-RAM radio-HPLC detector.

HPLC Purification of 7 for ^{64}Cu Radiolabeling. Purification of the macrobicyclic ligand **7** was performed on a Waters Empower^2 controlled Delta Prep HPLC including a Prep LC Controller, 717 Autosampler, Prep Degasser, and a 486 Tunable Absorbance Detector. Compound **7** (5 mg) was dissolved in the minimum volume of 1:1 acetonitrile: water and aliquots were injected into the HPLC system using an Atlantis PrepT3 10 μm OBD C-18 column (19 × 150 mm) running a gradient with the following conditions; 0−7 min, 20 mL/min, water (0.1% formic acid); 7−7.1 min 20−30 mL/min water (0.1% formic acid); 7.1−8 min 0−2% acetonitrile in water (0.1% formic acid) with monitoring absorbance at 210 nm. The peak at 7−8 min was collected in acid-washed glassware and evaporated to dryness (3.6 mg) under high vacuum and reconstituted in water (0.36 mL) for radiolabeling experiments.

^{64}Cu-10 Radiolabeling. To a 0.5 mL microcentrifuge tube was added an aqueous solution of macrobicyclic ligand **7** (10 μL of a 10 mg/mL solution; 100 μg), aqueous NH_4OAc (0.4 M, pH 5.5, 50 μL) and $^{64}CuCl_2$ in 0.02 M HCl, (20 μL, 23.1 MBq). The vial was then capped and the mixture heated at 85 °C for 1 h. The reaction mixture was injected into a preparative radio-HPLC system using an Atlantis Prep T3 5 μm C-18 column (10 × 250 mm) running a gradient with the following conditions; 0−10 min, 2.5 mL/min 5% acetonitrile in water (0.1% formic acid); 10−11 min, 5−50% acetonitrile in water (0.1% formic acid) and the radio-peak at 7.46 min was collected, and evaporated to dryness under high vacuum, yielding 16.07 MBq, 75.7% decay corrected yield from 93 min operation.

^{64}Cu-10 Stability Studies. In 0.5 mL microcentrifuge tubes ^{64}Cu-**10** (1.3 MBq) was incubated in phosphate buffered saline (PBS) (pH = 7.4, 222 μL) or in PBS with either L-cysteine or L-histidine (1×10^{-3} M, pH = 7.4, final volume = 222 μL) for 24 h at 37 °C. Stability was determined at 6 and 24 h time-points by injections on a radio-HPLC system and comparing the radiochemical purity.

Synthesis. 6. To a solution of tame (**S3**) (2.00 g, 0.017 mol) in chloroform (50 mL) under an atmosphere of N_2, was added an aqueous solution of K_2CO_3 (1.0 M, 50 mL). The mixture was cooled to 0 °C and, with vigorous stirring, a solution of 2-chloroacetyl chloride (4.06 mL, 0.051 mol) in chloroform (50 mL) was added dropwise. After 2 h, the mixture was warmed to room temperature (RT), and the organic phase was separated and washed with water (2 × 20 mL) and then dried with $MgSO_4$. The solvent was removed on the rotary evaporator, yielding the crude product as a pale yellow solid.

dx.doi.org/10.1021/ic4024508 | Inorg. Chem. 2014, 53, 468−477

The crude product was purified on silica using an eluent composed of 4:1 chloroform:methanol +25% aqueous ammonia solution (20 drops/100 mL), affording **6** as an off-white solid. Yield: 4.44 g, (75.1%). ^{1}H NMR (500 MHz, $CDCl_3$): δ 0.86 (s, 3H, CH_3, [H1]), 3.049 (d, 6H, $^3J_{HH}$ = 6.5 Hz, CH_2, [H3]), 4.08 (s, 6H, CH_2, [H6]), 7.78 (t, 3H, $^3J_{HH}$ = 6.5 Hz, CONH, [H4]) ppm. ^{13}C NMR ($CDCl_3$): δ 19.1 (C1), 41.6 (C2), 42.8 (C6), 43.2 (C3), 168.2 (C5) ppm. ESI-MS: m/z = 346.1 (H^+) calcd. For $C_{11}H_{19}N_3O_3Cl_3$ = 346.04. Found: C, 38.07; H, 5.34; N, 12.25%. $C_{11}H_{18}Cl_3N_3O_3$ requires C, 38.11; H, 5.23; N, 12.12%.

7. To a solution of **6** (1.07 g, 3.07 mmol) and tame (**S3**) (0.36 g, 3.07 mmol) in anhydrous acetonitrile (500 mL) under an atmosphere of N_2 was added K_2CO_3 (2.54 g, 18.4 mmol). The resulting solution was heated at 110 °C for 11 days. The solution was filtered while hot, and the solvent was removed on the rotary evaporator to afford a colorless oil. The crude product was purified on silica using an eluent composed of 4:1 chloroform: methanol +25% aqueous ammonia solution (20 drops/100 mL), affording **7** as a colorless oil that slowly crystallized. Yield: 0.122 g, (11.2%). ^{1}H NMR (500 MHz, $CDCl_3$): δ 0.86 (s, 3H, CH_3, [H1]), 0.88 (s, 3H, CH_3, [H10]), 1.86 (br, 3H, NH, [H7]), 2.62 (s, 6H, CH_2, [H8]), 3.25 (s, 6H, CH_2, [H6]), 3.43 (d, 6H, $^3J_{HH}$ = 7.0 Hz, CH_2, [H3]), 7.21 (t, 3H, $^3J_{HH}$ = 7.0 Hz, CONH, [H4]) ppm. ^{13}C NMR ($CDCl_3$): δ 21.7 (C10), 26.1 (C1), 38.5 (C2), 39.7 (C9), 49.7 (C3), 55.8 (C6), 59.3 (C8), 173.8 (C5) ppm. ESI-MS: m/z = 355.2 (H^+) calcd. For $C_{16}H_{31}N_6O_3$ = 355.24. Found: C, 52.60; H, 8.84; N, 22.67%. $C_{16}H_{30}N_6O_3{\cdot}0.6H_2O$ requires C, 52.61; H, 8.61; N, 23.01%.

8. This compound was prepared from **6** (1.09 g, 3.14 mmol), tacn (**S6**) (0.39 g, 3.14 mmol), and K_2CO_3 (2.61 g, 18.85 mmol) using the method described for **7**. Compound **8** was obtained as an off-white solid. Yield: 0.541 g, (47.0%). ^{1}H NMR (500 MHz, $CDCl_3$): δ 0.98 (s, 3H, CH_3, [H1]), 2.59−2.65 (m, 6H, CH_2, [H7a]), 2.80−2.86 (m, 6H, CH_2, [H7b]), 3.36 (s, 6H, CH_2, [H6]), 3.379 (d, 6H, $^3J_{HH}$ = 6.5 Hz, CH_2, [H3]), 7.92 (t, 3H, $^3J_{HH}$ = 6.5 Hz, CONH, [H4]) ppm. ^{13}C NMR ($CDCl_3$): δ 23.9 (C1), 39.8 (C2), 47.6 (C3), 53.5 (C7), 62.0 (C6), 171.4 (C5) ppm. ESI-MS: m/z = 367.2 (H^+) calcd. For $C_{17}H_{31}N_6O_3$ = 367.24. Found: C, 49.42; H, 7.53; N, 19.42%. $C_{17}H_{30}N_6O_3{\cdot}0.5CHCl_3$ requires C, 49.32; H, 7.21; N, 19.72%.

9. A stirred solution of **7** (50.0 mg, 0.141 mmol) and $CoCl_2.6H_2O$ (33.6 mg, 0.141 mmol) in water (10 mL) was aerated for 3 days, during which time the color changed from red to orange. The solution was filtered through a pad of Celite, and anionic and cationic species were removed by passing the reaction mixture through separate CM- and DEAE-Sephadex columns. The solvent was removed on the rotary evaporator to give an orange solid. The solid was triturated with chloroform (2 × 10 mL) followed by acetonitrile (3 × 10 mL), before being redissolved in ethanol (10 mL). The latter solution was filtered, and the solvent removed on the rotary evaporator to afford **9** as an orange solid. Yield: 6.0 mg, (10.4%). ^{1}H NMR (500 MHz, CD_3OD): δ 0.86 (s, 3H, CH_3, [H1]), 0.93 (s, 3H, CH_3, [H10]), 2.33 (d, 3H, $^2J_{HH}$ = 14.0 Hz, CH_2, [H8b]), 2.37 (d, 3H, $^2J_{HH}$ = 12.5 Hz, CH_2, [H3a]), 2.96 (d, 3H, $^2J_{HH}$ = 14.0 Hz, CH_2, [H8a]), 3.15 (d, 3H, $^2J_{HH}$ = 12.5 Hz, CH_2, [H3b]), 3.35 (d, 3H, $^2J_{HH}$ = 15.5 Hz, CH_2, [H6b]), 3.50 (d, 3H, $^2J_{HH}$ = 15.5 Hz, CH_2, [H6a]) ppm. ^{13}C NMR (CH_3OD): δ 21.2 (C1), 21.9 (C10), 42.4 (C9), 43.7 (C2), 51.9 (C3), 56.4 (C8), 62.2 (C6), 176.6 (C5) ppm. ESI-MS: m/z = 411.1 (H^+) calcd. For $C_{16}H_{28}N_6O_3Co$ = 411.15. Found: C, 46.39; H, 6.25; N, 20.59%. $C_{16}H_{27}N_6O_3Co.0.1H_2O$ requires C, 46.63; H, 6.65; N, 20.39%.

10. The pH of a solution of **7** (40.0 mg, 0.113 mmol) and $CuCl_2.2H_2O$ (19.2 mg, 0.113 mmol) in water (20 mL) heated to 50 °C was adjusted to pH ∼ 10 with an aqueous solution of NaOH (68 mM, 5 mL). After 1 h the solution was filtered and evaporated to dryness to afford a purple residue. The residual solid was extracted into ethanol (10 mL), and the resulting solution was filtered. The solvent was then removed on a rotary evaporator to give a purple solid. To remove residual NaCl, the ethanol extraction process was repeated 3 more times. The crude product was then recrystallized via the diffusion of vapors between a solution of the crude product in methanol and diethyl ether, affording **10** as a deep blue/purple crystalline solid. Yield: 23.5 mg, (50%). ESI-MS: m/z = 416.2 (H^+) calcd. For $C_{16}H_{29}N_6O_3Cu$ = 416.15. Found: C, 45.91; H, 7.00; N, 20.40%. $C_{16}H_{28}N_6O_3Cu$ requires C, 46.20; H, 6.78; N, 20.20%.

■ ASSOCIATED CONTENT

Ⓢ Supporting Information

Synthetic details for the preparation of the triamines: tame and tacn. ^{1}H and ^{13}C NMR spectra for **7** and **8** and compound numbering scheme used for ^{1}H and ^{13}C NMR assignment of **6**−**9**. Positive-ion ESI-mass spectrum for the Cu(II) complex **10** and UV−vis spectra for the reaction of cryptands **7** and **8** with $CuCl_2$. Additional X-ray crystallographic details for **6**−**10** and the ORTEP structure of compound **6**. Radio-HPLC chromatograms obtained at 6 and 24 h for a sample of ^{64}Cu-**10** incubated for 24 h in phosphate buffered saline (PBS, pH 7.4) and PBS with L-histidine and L-cysteine. This material is available free of charge via the Internet at http://pubs.acs.org.

■ AUTHOR INFORMATION

Corresponding Author

*E-mail: p.barnard@latrobe.edu.au. Fax: (+)61 3 9479 1266.

Notes

The authors declare no competing financial interest.

■ ACKNOWLEDGMENTS

We thank the Australian Research Council for ARC LIEF funding (LE100100109). The radiochemical work was financially supported by the Australian Institute of Nuclear Science and Engineering (AINSE), Lucas Heights Science & Technology Centre, New Illawarra Rd, Menai, N.S.W., 2234, Australia. ^{64}Cu radioisotope was kindly provided by Charmaine Jeffery of the RAPID Laboratories, Medical Technology and Physics, Sir Charles Gairdner Hospital, Nedlands, W.A., 6009, Australia.

■ REFERENCES

(1) Smith, S. V. *J. Inorg. Biochem.* **2004**, *98* (11), 1874−1901.
(2) Shokeen, M.; Anderson, C. J. *Acc. Chem. Res.* **2009**, *42* (7), 832−841.
(3) Anderson, C. J.; Ferdani, R. *Cancer Biother. Radiopharm.* **2009**, *24*, 379−393.
(4) Wadas, T. J.; Wong, E. H.; Weisman, G. R.; Anderson, C. J. *Chem. Rev.* **2010**, *110* (5), 2858−2902.
(5) Donnelly, P. S. *Dalton Trans.* **2011**, *40* (5), 999−1010.
(6) Holland, J. P.; Barnard, P. J.; Collison, D.; Dilworth, J. R.; Edge, R.; Green, J. C.; McInnes, E. J. L. *Chem.—Eur. J.* **2008**, *14* (19), 5890−5907.
(7) Holland, J. P.; Giansiracusa, J. H.; Bell, S. G.; Wong, L.-L.; Dilworth, J. R. *Phys. Med. Biol.* **2009**, *54* (7), 2103.
(8) Woodin, K. S.; Heroux, K. J.; Boswell, C. A.; Wong, E. H.; Weisman, G. R.; Niu, W.; Tomellini, S. A.; Anderson, C. J.; Zakharov, L. N.; Rheingold, A. L. *Eur. J. Inorg. Chem.* **2005**, *2005* (23), 4829−4833.
(9) Heroux, K. J.; Woodin, K. S.; Tranchemontagne, D. J.; Widger, P. C. B.; Southwick, E.; Wong, E. H.; Weisman, G. R.; Tomellini, S. A.; Wadas, T. J.; Anderson, C. J.; Kassel, S.; Golen, J. A.; Rheingold, A. L. *Dalton Trans.* **2007**, *0* (21), 2150−2162.
(10) Di Bartolo, N. M.; Sargeson, A. M.; Donlevy, T. M.; Smith, S. V. *J. Chem. Soc., Dalton Trans.* **2001**, *0* (15), 2303−2309.
(11) Di Bartolo, N.; Sargeson, A. M.; Smith, S. V. *Org. Biomol. Chem.* **2006**, *4* (17), 3350−3357.
(12) Voss, S. D.; Smith, S. V.; DiBartolo, N.; McIntosh, L. J.; Cyr, E. M.; Bonab, A. A.; Dearling, J. L. J.; Carter, E. A.; Fischman, A. J.; Treves, S. T.; Gillies, S. D.; Sargeson, A. M.; Huston, J. S.; Packard, A. B. *Proc. Natl. Acad. Sci.* **2007**, *104* (44), 17489−17493.

(13) Ma, M. T.; Karas, J. A.; White, J. M.; Scanlon, D.; Donnelly, P. S. *Chem. Commun.* **2009**, *0* (22), 3237−3239.
(14) Cooper, M. S.; Ma, M. T.; Sunassee, K.; Shaw, K. P.; Williams, J. D.; Paul, R. L.; Donnelly, P. S.; Blower, P. J. *Bioconjugate Chem.* **2012**, *23* (5), 1029−1039.
(15) Margerum, D. W.; Chellappa, K. L.; Bossu, F. P.; Burce, G. L. *J. Am. Chem. Soc.* **1975**, *97* (23), 6894−6896.
(16) Bossu, F. P.; Margerum, D. W. *J. Am. Chem. Soc.* **1976**, *98* (13), 4003−4004.
(17) Kirksey, S. T.; Neubecker, T. A.; Margerum, D. W. *J. Am. Chem. Soc.* **1979**, *101* (6), 1631−1633.
(18) Diaddario, L. L.; Robinson, W. R.; Margerum, D. W. *Inorg. Chem.* **1983**, *22* (7), 1021−1025.
(19) Collins, T. J.; Richmond, T. G.; Santarsiero, B. D.; Treco, B. G. R. T. *J. Am. Chem. Soc.* **1986**, *108* (8), 2088−2090.
(20) Anson, F. C.; Collins, T. J.; Richmond, T. G.; Santarsiero, B. D.; Toth, J. E.; Treco, B. G. R. T. *J. Am. Chem. Soc.* **1987**, *109* (10), 2974−2979.
(21) Collins, T. J.; Kostka, K. L.; Munck, E.; Uffelman, E. S. *J. Am. Chem. Soc.* **1990**, *112* (14), 5637−5639.
(22) Collins, T. J.; Kostka, K. L.; Uffelman, E. S.; Weinberger, T. L. *Inorg. Chem.* **1991**, *30* (22), 4204−4210.
(23) Bartos, M. J.; Gordon-Wylie, S. W.; Fox, B. G.; James Wright, L.; Weintraub, S. T.; Kauffmann, K. E.; Münck, E.; Kostka, K. L.; Uffelman, E. S.; Rickard, C. E. F.; Noon, K. R.; Collins, T. J. *Coord. Chem. Rev.* **1998**, *174* (1), 361−390.
(24) Liu, S. *Adv. Drug Delivery Rev.* **2008**, *60* (12), 1347−1370.
(25) Cantorias, M. V.; Howell, R. C.; Todaro, L.; Cyr, J. E.; Berndorff, D.; Rogers, R. D.; Francesconi, L. C. *Inorg. Chem.* **2007**, *46* (18), 7326−7340.
(26) O'malley, J. P.; Ziessman, H. A.; Chantarapitak, N. *Clin. Nucl. Med.* **1993**, *18* (1), 22−29.
(27) Antunes, P.; Delgado, R.; Drew, M. G. B.; Félix, V.; Maecke, H. *Inorg. Chem.* **2007**, *46* (8), 3144−3153.
(28) Barnard, P. J.; Holland, J. P.; Bayly, S. R.; Wadas, T. J.; Anderson, C. J.; Dilworth, J. R. *Inorg. Chem.* **2009**, *48* (15), 7117−7126.
(29) Cutler, C. S.; Wuest, M.; Anderson, C. J.; Reichert, D. E.; Sun, Y.; Martell, A. E.; Welch, M. J. *Nucl. Med. Biol.* **2000**, *27* (4), 375−380.
(30) Angus, P. M.; Elliott, A. J.; Sargeson, A. M.; Willis, A. C. *J. Dalton Trans.* **1999**, *7*, 1131−1136.
(31) Sargeson, A. *Chem. Br.* **1979**, *15* (1), 23−27.
(32) Bernhardt, P. V.; Bramley, R.; Engelhardt, L. M.; Harrowfield, J. M.; Hockless, D. C. R.; Korybut-Daszkiewicz, B. R.; Krausz, E. R.; Morgan, T.; Sargeson, A. M. *Inorg. Chem.* **1995**, *34* (14), 3589−3599.
(33) Motekaitis, R. J.; Sun, Y.; Martell, A. E.; Welch, M. J. *Can. J. Chem.* **1999**, *77*, 614−623.
(34) Sigel, H.; Martin, R. B. *Chem. Rev.* **1982**, *82* (4), 385−426.
(35) Farrugia, L. *J. Appl. Crystallogr.* **1997**, *30* (5 Part 1), 565.
(36) Bernhardt, P. V.; Bygott, A. M. T.; Geue, R. J.; Hendry, A. J.; Korybut-Daszkiewicz, B. R.; Lay, P. A.; Pladziewicz, J. R.; Sargeson, A. M.; Willis, A. C. *Inorg. Chem.* **1994**, *33* (20), 4553−4561.
(37) Geue, R.; Petri, W.; Sargeson, A.; Snow, M. *Aust. J. Chem.* **1992**, *45* (10), 1681−1703.
(38) Tang, J.-K.; Ou-Yang, Y.; Zhou, H.-B.; Li, Y.-Z.; Liao, D.-Z.; Jiang, Z.-H.; Yan, S.-P.; Cheng, P. *Cryst. Growth Des.* **2005**, *5* (2), 813−819.
(39) Achmatowicz, M.; Szumna, A.; Zieliński, T.; Jurczak, J. *Tetrahedron* **2005**, *61* (38), 9031−9041.
(40) Steggerda, J. J.; Bour, J. J.; Birker, P. J. M. W. L. *Inorg. Chem.* **1971**, *10* (6), 1202−1205.
(41) Wong, L. F.; Cooper, J. C.; Margerum, D. W. *J. Am. Chem. Soc.* **1976**, *98* (23), 7268−7274.
(42) Cai, H.; Fissekis, J.; Conti, P. S. *Dalton Trans.* **2009**, *27*, 5395−5400.
(43) Korybut-Daszkiewicz, B.; Klimkiewicz, J. *Chem. Commun.* **1996**, *10*, 1175−1176.
(44) Taylor, S.; Snow, M.; Hambley, T. *Aust. J. Chem.* **1983**, *36* (12), 2359−2368.
(45) Ma, M. T.; Cooper, M. S.; Paul, R. L.; Shaw, K. P.; Karas, J. A.; Scanlon, D.; White, J. M.; Blower, P. J.; Donnelly, P. S. *Inorg. Chem.* **2011**, *50* (14), 6701−6710.
(46) Fleischer, E. B.; Gebala, A. E.; Levey, A.; Tasker, P. A. *J. Org. Chem.* **1971**, *36* (20), 3042−3044.
(47) Beaufort, L.; Delaude, L.; Noels, A. F. *Tetrahedron* **2007**, *63* (30), 7003−7008.
(48) Hoveyda, H. R.; Karunaratne, V.; Nichols, C. J.; Rettig, S. J.; Stephens, A. K. W.; Orvig, C. *Can. J. Chem.* **1998**, *76* (4), 414−425.
(49) Madison, S. A.; Batal, D. J. Improved synthesis of 1,4,7-triazacyclononane, U.S. Patent US5284944 A, 1992.
(50) Barta, C. A.; Bayly, S. R.; Read, P. W.; Patrick, B. O.; Thompson, R. C.; Orvig, C. *Inorg. Chem.* **2008**, *47* (7), 2280−2293.
(51) *CrysAlisPro*, 171.35.11; Oxford Diffraction Ltd.: Abingdon, U.K., 2011.
(52) Sheldrick, G. M. *Acta Crystallogr., Sect. A* **2008**, *64* (1), 112−122.
(53) Dolomanov, O. V.; Bourhis, L. J.; Gildea, R. J.; Howard, J. A. K.; Puschmann, H. *J. Appl. Crystallogr.* **2009**, *42* (2), 339−341.